ESI to accompany

Manipulating connecting nodes through remote alkoxy chain variation in coordination networks with 4'-alkoxy-4,2':6',4''-terpyridine linkers

Y. Maximilian Klein, Alessandro Prescimone, Edwin C. Constable and Catherine E. Housecroft*

Figs. S1–S5: X-Ray powder diffraction data

Shifts between observed and theoretical peaks are due to the difference between the temperatures of the measurement (room temperature for powder and single crystal structures at 123 K).

Fig. S1. $[\{Cd_2(NO_3)_4(\mathbf{2})_3\}\cdot 3CHCl_3]_n$

Fig. S2. $[\{Cd_2(NO_3)_4(\mathbf{3})_4\}\cdot 3CHCl_3]_n$

Fig. S3. $[\{Cd_2(NO_3)_4(\mathbf{4})_4\}\cdot CHCl_3\cdot MeOH]_n$

Fig. S4. $[\{Cd(NO_3)_2(\mathbf{5})_2\}\cdot 2MeOH]_n$

Fig. S5. $[Cd_2(NO_3)_4(MeOH)(\mathbf{4})_3]_n$

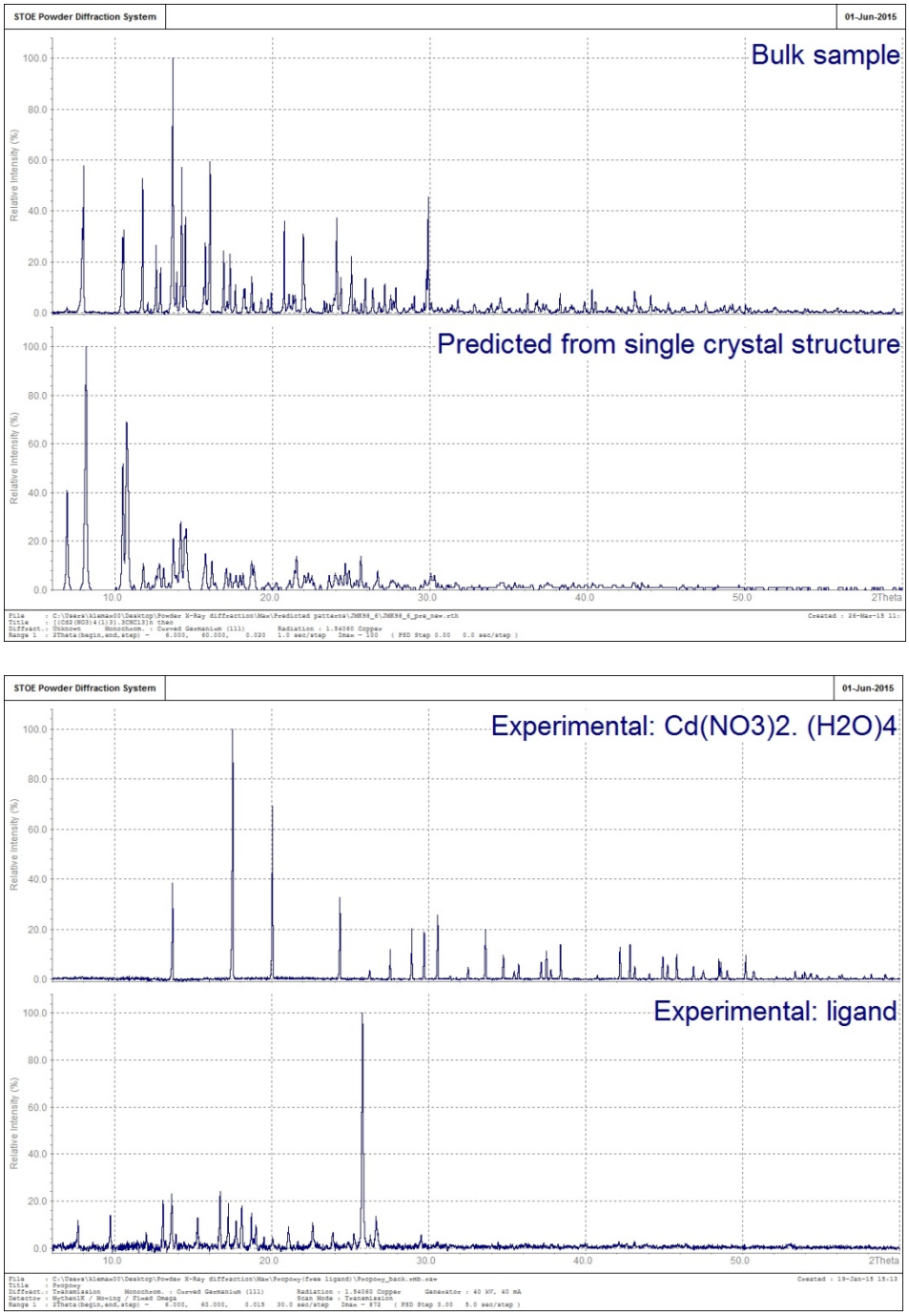

Fig. S1. X-ray powder diffraction patterns of the bulk sample of $[\{Cd_2(NO_3)_4(\mathbf{2})_3\}\cdot 3CHCl_3]_n$ (≈295 K) compared to the predicted pattern from the single crystal data (123 K) and to experimental powder patterns (≈295 K) for the precursors $Cd(NO_3)_2\cdot 4H_2O$ and ligand **2**.

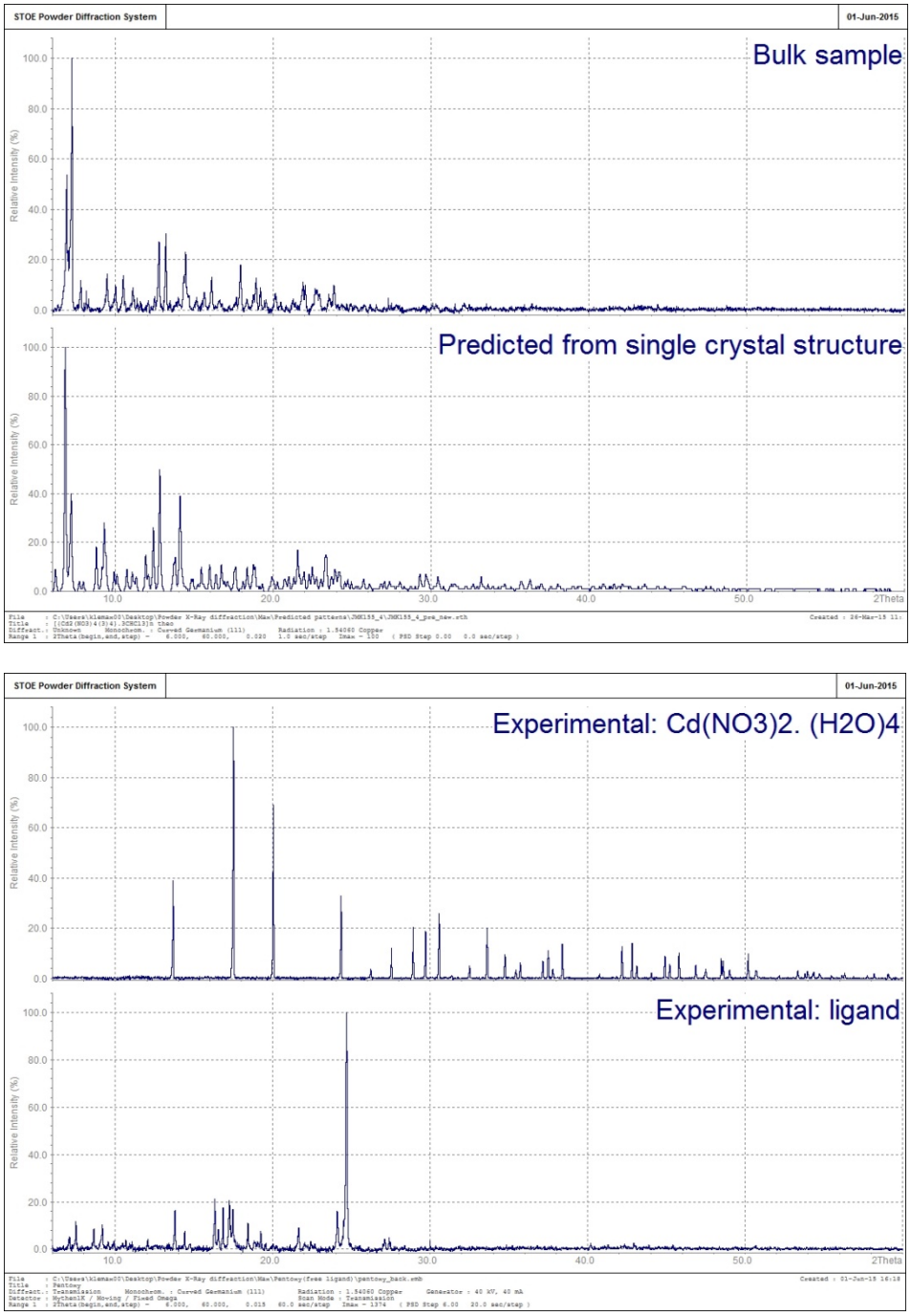

Fig. S2. X-ray powder diffraction patterns of the bulk sample of $[\{Cd_2(NO_3)_4(\mathbf{3})_4\}\cdot 3CHCl_3]_n$ (≈295 K) compared to the predicted pattern from the single crystal data (123 K) and to experimental powder patterns (≈295 K) for the precursors $Cd(NO_3)_2\cdot 4H_2O$ and ligand **3**.

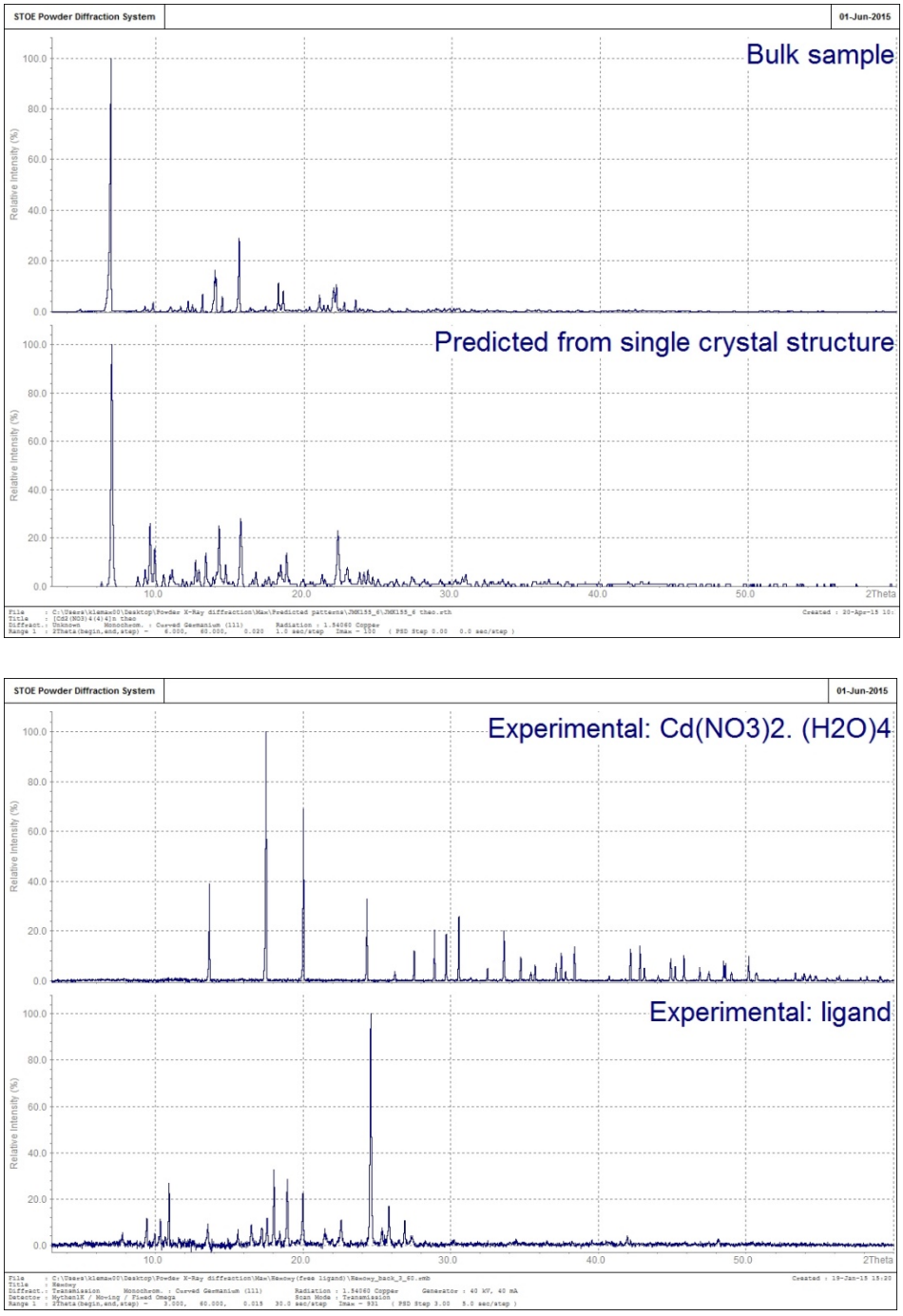

Fig. S3. X-ray powder diffraction patterns of the bulk sample of $[\{Cd_2(NO_3)_4(\mathbf{4})_4\}\cdot CHCl_3\cdot MeOH]_n$ (≈295 K) compared to the predicted pattern from the single crystal data (123 K) and to experimental powder patterns (≈295 K) for the precursors $Cd(NO_3)_2\cdot 4H_2O$ and ligand **4**.

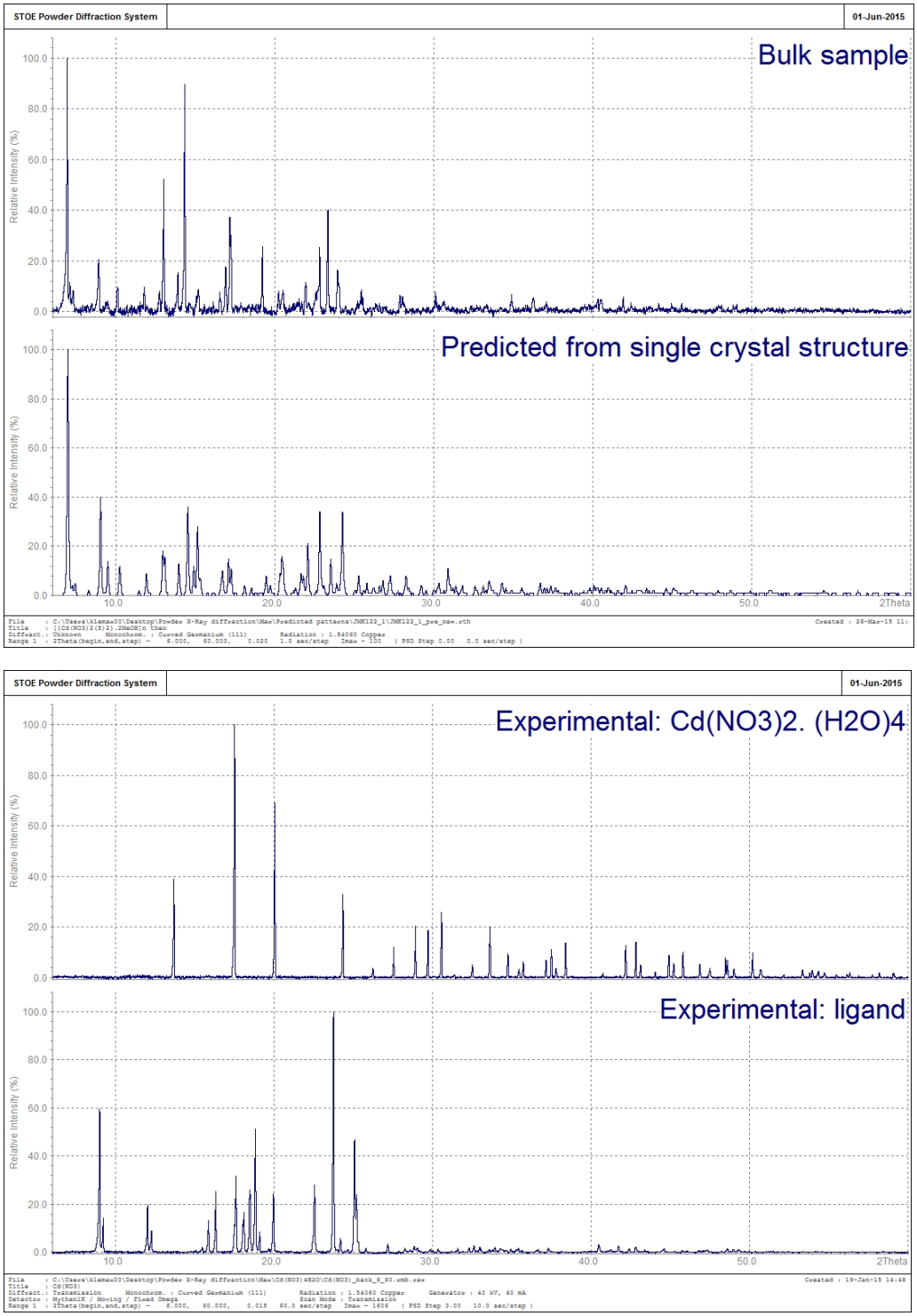

Fig. S4. X-ray powder diffraction patterns of the bulk sample of $[\{Cd(NO_3)_2(\mathbf{5})_2\}\cdot 2MeOH]_n$ (≈295 K) compared to the predicted pattern from the single crystal data (123 K) and to experimental powder patterns (≈295 K) for the precursors $Cd(NO_3)_2\cdot 4H_2O$ and ligand **5**.

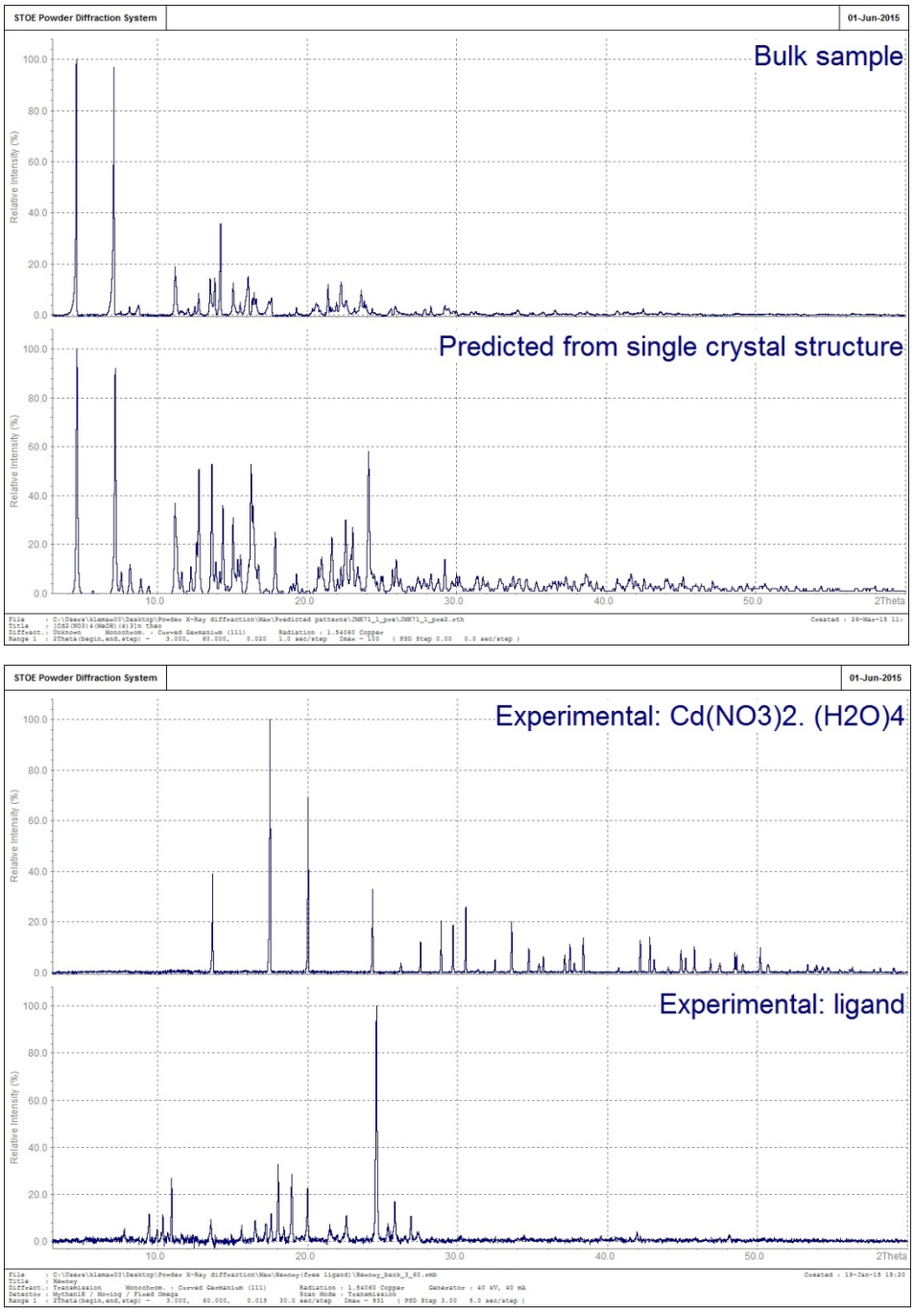

Fig. S5. X-ray powder diffraction patterns of the bulk sample of $[Cd_2(NO_3)_4(MeOH)(\mathbf{4})_3]_n$ (≈295 K) compared to the predicted pattern from the single crystal data (123 K) and to experimental powder patterns (≈295 K) for the precursors $Cd(NO_3)_2{\cdot}4H_2O$ and ligand **4**.

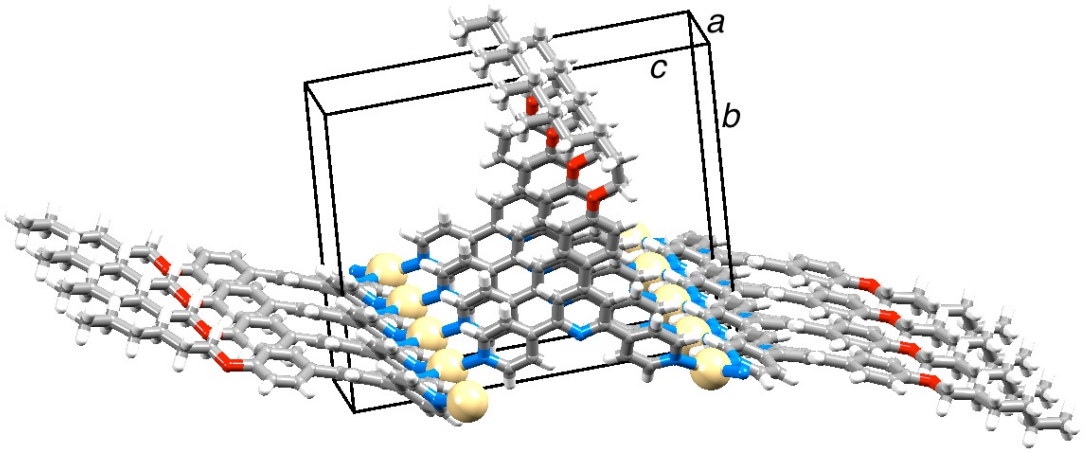

Fig. S6. Part of one ladder in the 1-dimensional coordination polymer $[Cd_2(NO_3)_4(MeOH)(\mathbf{4})_3]_n$; the ladder follows the *a*-axis. Nitrato amd MeOH ligands are omitted for clarity.